



Influence of gas injection location and magnetic perturbations on ICRF antenna performance in ASDEX Upgrade

V. Bobkov, I. Stepanov, P. Jacquet, I. Monakhov, R. Bilato, L. Colas, A. Czarnecka, R. Dux, H. Faugel, A. Kallenbach, H. W. Müller, J.-M. Noterdaeme, S. Potzel, Th. Pütterich, W. Suttrop, and ASDEX Upgrade team

Citation: *AIP Conference Proceedings* **1580**, 271 (2014); doi: 10.1063/1.4864540

View online: <http://dx.doi.org/10.1063/1.4864540>

View Table of Contents: <http://scitation.aip.org/content/aip/proceeding/aipcp/1580?ver=pdfcov>

Published by the [AIP Publishing](http://aip.org)

Articles you may be interested in

[A multichannel reflectometer for edge density profile measurements at the ICRF antenna in ASDEX Upgrade](#)
AIP Conf. Proc. **1580**, 566 (2014); 10.1063/1.4864614

[Density profile sensitivity study of ASDEX Upgrade ICRF Antennas with the TOPICA code](#)
AIP Conf. Proc. **1406**, 93 (2011); 10.1063/1.3664936

[Electromagnetic simulations of the ASDEX Upgrade ICRF Antenna with the TOPICA code](#)
AIP Conf. Proc. **1187**, 137 (2009); 10.1063/1.3273712

[Status and development of the ICRF antennas on ASDEX Upgrade](#)
AIP Conf. Proc. **694**, 154 (2003); 10.1063/1.1638017

[Achievement of the Hmode with a screenless ICRF antenna in ASDEX Upgrade](#)
AIP Conf. Proc. **355**, 47 (1996); 10.1063/1.49511

Influence of Gas Injection Location and Magnetic Perturbations on ICRF Antenna Performance in ASDEX Upgrade

V. Bobkov^a, I. Stepanov^{a,b}, P. Jacquet^c, I. Monakhov^c, R. Bilato^a, L. Colas^d,
 A. Czarnecka^c, R. Dux^a, H. Faugel^a, A. Kallenbach^a, H. W. Müller^a,
 J.-M. Noterdaeme^{a,b}, S. Potzel^a, Th. Pütterich^a, W. Suttrop^a and ASDEX Upgrade team

^aMax-Planck-Institut für Plasmaphysik, EURATOM-Association, D-85748, Germany

^bDepartment of Applied Physics, Gent University, 9000 Gent, Belgium

^cEuratom/CCFE Fusion Association, Culham Science Centre, Abingdon, OX14 3DB, UK

^dCEA, IRFM, 13108 Saint Paul-lez-Durance, France

^eInstitute of Plasma Physics and Laser Microfusion, Association EURATOM-IPPLM, Warsaw, Poland

Abstract. In ASDEX Upgrade H-modes with $H_{98} \approx 0.95$, similar effect of the ICRF antenna loading improvement by local gas injection was observed as previously in L-modes. The antenna loading resistance R_a between and during ELMs can increase by more than 25% after a switch-over from a deuterium rate of $7.5 \cdot 10^{21}$ D/s injected from a toroidally remote location to the same amount of deuterium injected close to an antenna. However, in contrast to L-mode, this effect is small in H-mode when the valve downstream w.r.t. parallel plasma flows is used. In L-mode, a non-linearity of R_a at $P_{ICRF} < 30$ kW is observed when using the gas valve integrated in antenna. Application of magnetic perturbations (MPs) in H-mode discharges leads to an increase of $R_a > 30\%$ with no effect of spectrum and phase of MPs on R_a found so far. In the case ELMs are fully mitigated, the antenna loading is higher and steadier. In the case ELMs are not fully mitigated, the value of R_a between ELMs is increased. Looking at the W source modification for the improved loading, the local gas injection is accompanied by decreased values of tungsten (W) influx Γ_W from the limiters and its effective sputtering yield Y_W , with the exception of the locations directly at the antenna gas valve. Application of MPs leads to increase of Γ_W and Y_W for some of the MP phases. With nitrogen seeding in the divertor, ICRF is routinely used to avoid impurity accumulation and that despite enhanced Γ_W and Y_W at the antenna limiters.

Keywords: ASDEX Upgrade, ICRF, antenna, coupling, sputtering.

PACS: 52.50.G, 52.40.F, 52.40.H

INTRODUCTION AND EXPERIMENTAL SETUP

For a variety of conditions in ITER, Ion Cyclotron Range of Frequencies (ICRF) antennas can have limitations to couple 20 MW per antenna [1]. Application of standard ICRF coupling techniques, such as reduction of the plasma-antenna clearance and the global increase of the density, will be limited due to machine protection and plasma scenario limitations. It is therefore important to explore alternative possibilities to improve ICRF coupling performance. At the same time an eye should be kept on changes in the impurity production associated with those. Two additional methods to improve ICRF antenna loading can be utilized in ASDEX Upgrade. First, as has been previously shown [2] for L-mode discharges, the coupling resistance of ICRF antennas can be substantially increased by using deuterium gas valves which are located near the antennas. Second, operation of the in-vessel magnetic perturbation (MP) coils of ASDEX Upgrade (AUG), the so-called B-coils [3], is often accompanied by an increased density at the plasma edge [4] and can be used to improve the antenna loading [5].

Fig. 1 shows the ICRF antennas, midplane gas valves and the relevant local diagnostics. Four ICRF antennas ($a1$ to $a4$, operated in pairs $a1/a3$ and $a2/a4$ within the 3dB hybrid scheme unless mentioned otherwise) were used with the hydrogen minority heating in deuterium for the experiments considered. Standard RF signals provide measurements of antenna resistance R_a averaged over both antenna feeders, Li-beam provides density profile at the edge and limiter spectroscopy monitors deuterium and tungsten (W) influxes. Gas valves in sector 1 and sector 13 are recessed and allow a toroidal and poloidal spread of neutrals before ionization. Neutrals from the antenna valve are injected at the limiter and are ionized close to the injection point. Compared to the setup from [2], the antenna valve was relocated from $a4$ to $a3$. It was found that, in

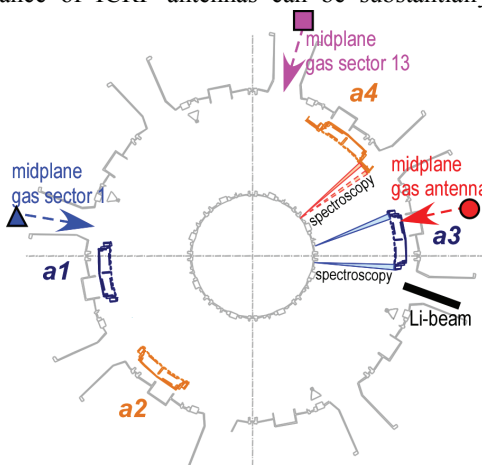


FIG. 1. AUG toroidal view of ICRF antennas, midplane gas valves and relevant diagnostics.

contrast to $a4$ in 2009, $a3$ with the optically closed Faraday Screen (FS) has the upper limitation on the gas injection rate from the antenna valve of $\approx 10^{22}$ deuterons (D)/s. At this limit, $a3$ starts arcing at low power (< 50 kW) and at high power (> 200 kW), supposedly due to the limited pumping through the optically closed FS.

ANTENNA LOADING IMPROVEMENT

A repeat of the L-mode discharges from [2] with the total gas rate of $7.5 \cdot 10^{22}$ D/s reproduced the same findings about the effect of local gas from midplane on the antenna loading: R_a of $a1$, $a3$ and $a4$ increase significantly when the local gas valve is utilized instead of remote gas injection with the same rate. However, even with the different arrangement of the antenna valve (at $a3$ instead of that at $a4$ in 2009) w.r.t. the Li-beam diagnostics, an effect on the density profile in the scrape-off layer (SOL) is not distinguishable when using the antenna gas valve. Thus, measurements of the density profiles in several locations in front of the antennas are necessary. These should be available in the future [6]. Presently, spectroscopy measurements on the lines of sight (LOSs) looking at both sides of $a3$ confirm that the increase of deuterium influx after the switch-over from the valve in sector 1 to the antenna valve is localized poloidally and toroidally at the locations directly at the antenna valve injectors. Other LOSs at $a3$ show small changes of deuterium influx.

For characterization of R_a in H-mode, discharges #29477 and #29514 were used with $P_{NBI}=5$ MW, $P_{ICRF}=1.5$ MW at 30 MHz and $B_r=-2.0$ T, gas rate of $7.5 \cdot 10^{21}$ D/s. The waveforms of the ICRF power toggling between the antenna pairs and the scan of antenna-separatrix clearance at midplane Δr were similar to [2]. The discharges were stable, with $n_e=6.5 \cdot 10^{19}$ m $^{-3}$ line average density on the central line of sight of DCN interferometer and the H-mode performance of $H_{98}\approx 0.95$. Fig.2 shows time-averaged R_a for each antenna between and during ELMs depending on Δr for the conditions when the whole gas injection is performed from a single midplane valve, for different valves. Fig.2 uses the color and the symbol coding for the gas valves as shown in Fig.1. For $a1$ and $a3$, at least 25% of R_a between ELMs can be gained when using the sector 1 valve or the antenna valve respectively. For R_{a1} and R_{a3} during ELMs, the difference between the valves is higher (up to 50 %). Interestingly, in contrast to the L-mode discharges, $a4$ shows very little improvement when local gas valve at sector 13 is used. Thus the toroidal proximity of gas valve [2] is not the only important parameter for gas valve placement needed to achieve the ICRF loading improvement in H-mode. The side where the valve is placed toroidally w.r.t. antenna can obviously play a role. One of the explanations of this could be an influence of the parallel plasma flows on the build-up of the density profile in front of the antennas. Assuming the parallel flow pattern is as described in [7] for AUG, the sector 13 gas valve (with a small effect on R_{a4}) is located downstream (i.e. towards flow direction) w.r.t. $a4$, whereas the sector 1 gas (with a significant effect on R_{a1}) is located upstream w.r.t. $a1$. The smaller effect on R_{a4} in H-mode could also be influenced by the unique design of $a4$ which is the antenna with broad limiters and narrower straps [8]. It is noteworthy, that for the cases of remote gas injection, similar R_a is observed for each antenna, with R_{a4} being marginally lower.

The use of logarithmic RF detectors [9] made possible the measurements of the RF power dependence of R_a in the low power range and thus a characterization of the antenna loading non-linearity. The data for the L-mode discharge #29472 is presented in Fig.3. The discharges had synchronous replacement of the power from one antenna pair by the power from another antenna pair to keep the total heating power $P_{heat}=P_{ICRF}=1$ MW and the central plasma parameters constant. A small influence of the local

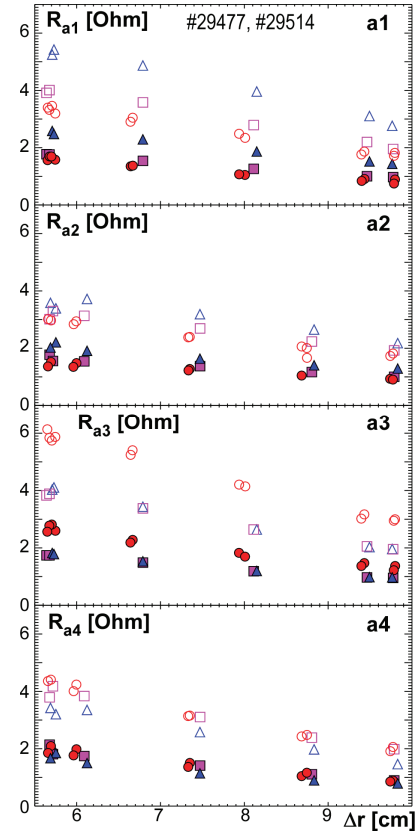


FIG. 2. Time-averaged R_a between ELMs (filled) and during ELMs (hollow) vs. Δr for all antennas. Colors and symbols for gas valves are as in Fig.1.

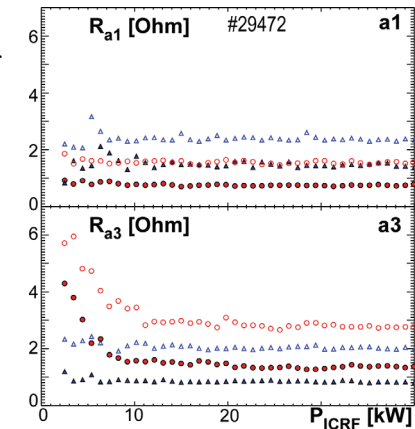


FIG. 3. R_a vs. RF power in L-mode for $a1$ and $a3$ for $\Delta r=6$ cm (hollow) and $\Delta r=10.5$ cm (filled). Colors and symbols for gas valves are as in Fig.1.

gas injection on the power dependence of R_a is present for $a1$, whereas a large influence is observed for $a3$ when the valve in the antenna is used. For the latter case R_a is strongly non-linear at $P_{ICRF} < 30$ kW. This could be interpreted as a sign of the local gas ionization by RF fields in front of the antennas: a rough estimate of the maximum power required to ionize $7.5 \cdot 10^{21}$ D/s yields 40 kW and would be compatible with the observed picture. However other effects like multipactor, RF sheath losses and density depletion due to the $E \times B$ convection and due to the ponderomotive effect can take part in producing a similar dependency. In addition, at least a part of the interactions is likely to happen inside the antenna box and/or in the vacuum transmission lines, because of the increased arcing probability at low power levels (as mentioned above), supposedly aided by the multipactor-assisted ionization at the observed RF voltages below 3 kV.

Generally in H-modes, the MP coils influence R_a positively. Operation of the coils in high density H-mode discharges influences ELM behavior as well as the density profile. So far no distinguishable influence of the spectrum or the phase of the coils on the loading was found. In the case of ELM mitigation, antenna loading is higher and much steadier [9]. In the case when ELMs are not mitigated or mitigated partially, averaged R_a between ELMs increases, as can be seen in Fig. 4, for $a1$ and $a2$ in #29863 with $P_{NBI} = 5$ MW, $P_{ICRF} = 1.5$ MW at 30 MHz with all antennas powered simultaneously, $B_T = 2.0$ T, $n_e = 9.5 \cdot 10^{19} \text{ m}^{-3}$, $n = 2$ for B-coils at 1 kA, with gas rate of $2.5 \cdot 10^{22}$ D/s, all injected from the divertor. The effect can be reproduced relatively well by R_a calculated by the FELICE code with real plasma profiles averaged in time in the code's input (see Fig. 4). Some scatter in the FELICE results is present due to the ELM-like events between ELMs influencing the measured profiles in the SOL. Best agreement of FELICE is observed with $a2$. The latter shows a difference to $a1$ at these high gas injection rates, despite the fact that gas injection from the divertor is used. This implies that there are density profile asymmetries in front of the antennas under these conditions as well.

TUNGSTEN SOURCE WITH IMPROVED LOADING AND N_2 -INJECTION

Local gas injection can affect the ICRF specific W source from the antenna limiters. The latter is characterized by intensity of the WI spectral line at 400.9 nm, with the time resolution of 3.4 ms. In L-mode discharges, $a4$ experiences typically a reduction of W influx Γ_W and effective W sputtering yield $Y_W = \Gamma_W / \Gamma_D$ when the sector 13 gas valve is used [10]. A similar effect, but smaller and with larger oscillations due to ELMs is present in H-mode discharges.

When the gas is injected from the antenna valve in $a3$, the W source distribution at the limiters of this antenna is affected significantly. General tendency is reflected in Fig. 5 for the H-mode discharge #29477. During the switch-over of the gas injection from the sector 1 valve to the $a3$ antenna valve, values Y_W and Γ_W , averaged over multiple ELM periods during $a3$ operation, are decreased at the LOSs which look at the limiters areas further away from the valve injectors (solid lines) for small Δr . At the same time, at the LOSs which look directly at the injectors, Y_W and Γ_W are strongly increased (dashed lines) for all Δr . This indicates that integrating a gas valve inside the antenna is not the best option in terms of impurity production. A valve near antenna results in consistently better behavior impurity wise. Unfortunately no spectroscopy measurements are available at $a1$ where the benefit of local gas injection from the valve near antenna is largest in H-mode discharges.

It has been previously observed [11] that the precise configuration of magnetic field lines and their connection lengths is important for the W source during ICRF. It is therefore interesting if MPs have an effect on the W source. An example of the effect of MPs on the W production on $a3$ is shown in Fig. 6, where the dependencies of Y_W and Γ_W between ELMs vs. Δr are presented for different phases of MPs (polarity of B-coils [3] is indicated in the figure) and the cases without MPs for #29863. All antennas are powered simultaneously, and Y_W and Γ_W are shown on the LOSs at $a3$ which are not connected to other antennas along the magnetic field lines. It

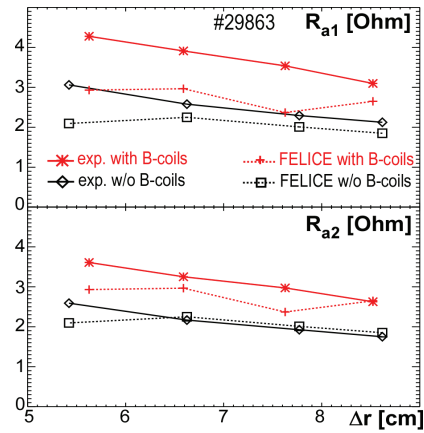


FIG. 4. Time-averaged R_a between ELMs at $a1$ and $a2$ vs. Δr (solid) for the cases with B-coils and without B-coils and comparison to R_a calculated by FELICE (dotted).

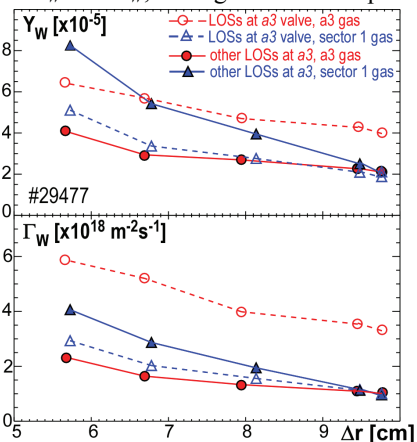


FIG. 5. Y_W and Γ_W vs. Δr at spectroscopy LOSs looking directly at the $a3$ injectors (dashed) and the $a3$ LOSs looking further away from injectors (solid).

can be seen that some of the phases of MPs produce a moderate increase of the W source. Such reaction is similar to the reaction during reduction of Δr . Fig.6 encourages further studies of the influence of MPs on the W source and its distribution at the antenna limiters, in particular in L-mode shots with discrete antenna powering.

The effect of N₂ on the ICRF performance is important to look at, especially in the context of the success of radiative scenarios in AUG [12]. Whereas dosing the N₂ injection from the midplane to test a possible effect on antenna loading has proved difficult, N₂ divertor injection is used regularly with ICRF which provides central heating to avoid impurity accumulation in the plasma center. Fig.7 summarizes findings for W concentration c_W measured close to $T_e=1.5$ keV using quasi-continuum spectral lines of highly charges W ions, and averaged Y_W and Γ_W at all LOSs looking at the limiters of $a3$ and $a4$. Phases with $a1/a2$ (boron coated limiters) and $a3/a4$ antenna (W coated limiters) pairing are distinguished. Fig. 7 shows that the W sputtering at the limiters is enhanced by N₂ at low and at high injection rates. Here the W source grows continuously with the increase of N₂ injection rate. However, c_W experiences a drop at higher level of N₂ injection. This is connected rather to a transport effect than to the W source effect.

CONCLUSIONS

AUG data shows that the local deuterium injection can increase the ICRF antenna loading significantly both in L-mode and in H-mode discharges. In H-mode discharges, the toroidal proximity of gas valve w.r.t. antenna is not the only parameter describing the potential benefit of the loading improvement. The data suggests that the location w.r.t. the upstream or downstream sides of the SOL parallel plasma flows can be important. The antenna valve with injectors close to the ionization zone leads to a very local ionization near antenna and to enhanced non-linear antenna-plasma interactions. A more favorable solution in AUG is the midplane valve next to antenna with injectors radially retracted. Such valve has the positive effect on the loading without the drawbacks of increased arcing probability and increased local impurity source and even with a positive effect on the latter. MP coils can improve the antenna loading by increasing the density profiles at the plasma edge. The accompanying modification of W source is moderate and should be studied more in details in the future. Injection of N₂ can be successfully used with ICRF despite the enhanced W source.

Acknowledgements. This work, supported by the European Communities under the contract of Association between EURATOM, CCFE and IPP Garching, was carried out within the framework of EFDA task WP12-IPH-A11-3-05/PS. The views and opinions expressed herein do not necessarily reflect those of the European Commission.

REFERENCES

1. A. Messiaen et al., *Nucl. Fusion* **50** (2010) 025026
2. P. Jacquet et al., *Nucl. Fusion* **52** (2012), 042002.
3. W. Suttrop et al., *Phys. Rev. Lett.* **106**, 22 (2011), 225004.
4. H.W. Müller et al., *J. Nucl. Mater.*, **438** (2013), S64-S71.
5. I. Stepanov et al., this conference.
6. O. Tudisco et al, this conference.
7. H.W. Müller et al., *J. Nucl. Mater.* **363-365** (2007), 605-610.
8. V. Bobkov et al., *Nucl. Fusion* **50** (2010) 035004.
9. H. Faugel et al., this conference.
10. V. Bobkov et al., submitted to *Nucl. Fusion*.
11. V. Bobkov et al. *J. Nucl. Mater.* **415**, 1 (2011) S1005-S1008.
12. A. Kallenbach et al., *Nucl. Fusion* **52** (2012) 122003.

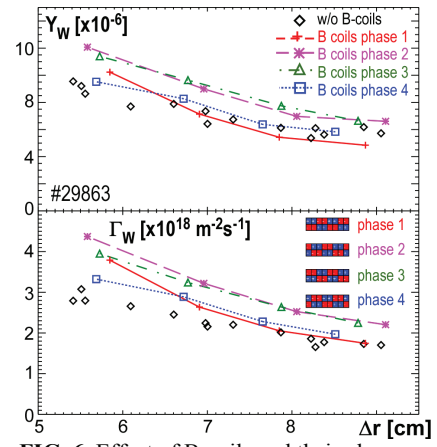


FIG. 6. Effect of B-coils and their phase on Y_W and Γ_W between ELMs at $a3$ LOSs not connected to other antennas along field lines.

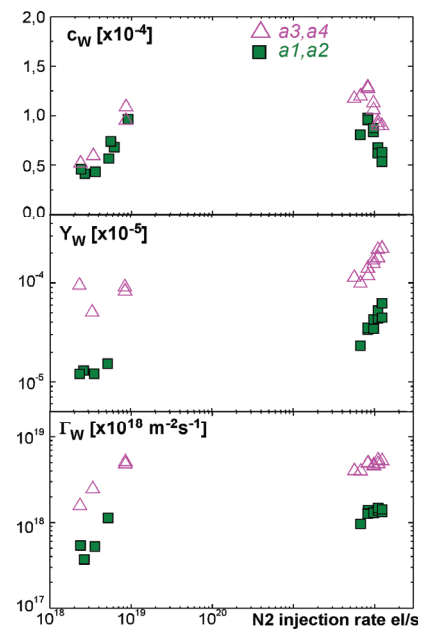


FIG. 7. Effect of N₂ injection on c_W , Y_W and Γ_W in discharges with high P_{heat} including $P_{ICRF}=2$ MW.